Available online at www.sciencedirect.com

SciVerse ScienceDirect

Journal of the European Ceramic Society 32 (2012) 787–793

www.elsevier.com/locate/jeurceramsoc

Zircon–zirconia ($ZrSiO_4$–ZrO_2) dense ceramic composites by spark plasma sintering

Nicolas M. Rendtorff [a,b,c,*], Salvatore Grasso [c], Chunfeng Hu [c,d], Gustavo Suarez [a,b], Esteban F. Aglietti [a,b], Yoshio Sakka [c,d]

[a] *Centro de Tecnología de Recursos Minerales y Cerámica (CETMIC): (CIC-CONICET-CCT La Plata), Camino Centenario y 506, C.C. 49, M.B. Gonnet, B1897ZCA Buenos Aires, Argentina*

[b] *Facultad de Ciencias Exactas, Universidad Nacional de La Plata, 47 y 115 La Plata, Buenos Aires, Argentina*

[c] *Fine Particle Processing Group, Nano Ceramics Center, National Institute for Materials Science (NIMS), 1-2-1 Sengen, Tsukuba, Ibaraki 305-0047, Japan*

[d] *WPI-MANA World Premier International Research Center Initiative, Center for Materials Nanoarchitectonics, NIMS, 1-2-1 Sengen, Tsukuba, Ibaraki 305-0047, Japan*

Received 21 January 2011; received in revised form 2 October 2011; accepted 16 October 2011
Available online 6 November 2011

Abstract

Dense reinforced zircon ($ZrSiO_4$)–20 vol.% zirconia (ZrO_2) ceramic composites were obtained by spark plasma sintering (SPS) starting from high energy milled commercially available powders. The sintering temperature and holding time resulted in two different microstructural configurations.

In the first configuration, the nano sized zirconia nanoparticles (100 nm) act as a bonding phase continuously dispersed along the zircon micronic (1–4 μm) grains. In the second one, a continuous zircon phase with well dispersed zirconia grains was achieved.

Both configurations led to improvement in fracture toughness and Vickers hardness if compared to pure zircon material processed under the same sintering condition. By comparing the developed microstructure configurations, the second one exhibits higher fracture toughness (almost 4.0 MPa $m^{1/2}$) due to the more effective zirconia reinforcement effects.

Keywords: Zircon; Zirconia; Composites; Sintering

1. Introduction

Nowadays composite and nanocomposite materials have found important industrial and technological applications. The properties of the resulting in the nanosized composite are not necessarily comparable to the ones of original materials.[1–3] The introduction of a second phase makes the material microstructure design more flexible. In ceramic materials the microstructure and properties are highly controllable by the processing, the microstructure design and chemical composition of the starting powders.

Unlike conventional methods like pressureless sintering and hot-pressing, spark plasma sintering (SPS), a high density current activated sintering method, permits to lower the sintering temperature and shorter the holding time, resulting in a remarkable improvements in properties of materials consolidated by this method. SPS has been demonstrated efficient technique to fully densify nanometric powders with negligible grain growth.[4–6]

In order to obtain well dispersed nanocomposite powder mixture several techniques have been proposed in order to overcome the spontaneous agglomeration of nano sized particle mixture. Some methods are based on aqueous nanoparticles dispersion under untrasonification with optimized selection of dispersant and pH concentrations.[7,8] The particles deagglomeration permits to achieve homogeneus mixture with inherent benefits of the nanostructured bulk materials.[7,8]

The high energy ball milling (HEBM) is effective to obtain uniform powder mixtures even in the case of nanosized powders. It promotes the mechanochemical activation which has proved to promote the solid-state reaction at low temperatures.[9] The "mechanical" effects of milling, such as the reduction

* Corresponding author at: Centro de Tecnología de Recursos Minerales y Cerámica (CETMIC): (CIC-CONICET-CCT La Plata), Camino Centenario y 506, C.C. 49, M.B. Gonnet, B1897ZCA Buenos Aires, Argentina.
Tel.: +54 221 4840247; fax: +54 221 4710075.
E-mail address: rendtorff@cetmic.unlp.edu.ar (N.M. Rendtorff).

0955-2219/$ – see front matter © 2011 Elsevier Ltd. All rights reserved.
doi:10.1016/j.jeurceramsoc.2011.10.021

of particle size and the mentioned mixture homogenization, are combined with chemical effects. The HEBM followed by SPS, has proved to process dense nanostructured ceramic composites.[10–13]Zircon ($ZrSiO_4$) is an excellent refractory material, it does not undergo to any structural transformation up to its dissociation temperature (1675 °C). It exhibits several attractive properties for high temperature structural applications such as excellent chemical stability, low thermal expansion coefficient and low heat conductivity. Zircon is employed in severe conditions requiring high temperature stability, high chemical inertness together with thermal shock resistance.[14–16]

Zircon ceramic posses moderately low flexural strength, hardness, and fracture toughness in the ranges of 200–300 MPa; 10–11 GPa; 2–3 MPa $m^{1/2}$ respectively.[14,17,18] In our recent work,[13] the mechanical properties of pure zircon were enhanced significantly (Hv 13.7 GPa and K_{IC} 3.6 MPa $m^{1/2}$) by the application of the advance ceramic processing employed in the present article as well. However, on absolute value, the mechanical properties of zircon are lower than other engineered ceramics such as tetragonal zirconia polycrystal (TZP) and Si_3N_4. Thus, it is of great importance to fabricate zircon composites by incorporating a reinforcing phase to improve the mechanical properties especially under high corrosion environment.

Several approaches have been used to improve the mechanical properties of zircon by the incorporating a second and third phases as SiC, TiC, partially stabilized zirconia, mullite, etc.[18–28] Focus in the microstructural configuration of these materials was particularly studied, in fact the effect of fibres and whiskers incorporation in zircon matrix were investigated.[21,22,25,26] The mechanical and fracture properties of the zircon material were improved by the incorporation of mullite and electro-fused mullite zirconia grains to zircon materials.[27,28] The direct influence of the zirconia (monoclinic) content in the improvement was established.[27,28]

Particularly zirconia incorporation promotes enhancement of toughness trough several concurring mechanisms. Different mechanisms are involved in the toughening: stress-induced transformation, microcraking, crack bowing and crack deflection and also the thermal expansion mismatch. In all cases, the operative toughening mechanism is controlled by matrix stiffness, zirconia particle size, chemical composition and testing temperature.[29–32]

In the present work several dense zircon–zirconia (monoclinic) composite materials were processed by SPS starting from high energy ball milling (HEBM) of the zircon and nanosized monoclinic zirconia powders. The ratio between the particle sizes of the two starting materials was about ten to one.

2. Experimental procedures

Recently we successfully produced pure dense zircon ceramics from mechanically activated powders followed by spark plasma sintering (SPS).[13] In order to easily compare the effect of the zirconia addition, the processing conditions in both investigations were keep identical.

The zircon starting powder was zirconium silicate with ZrO_2 = 64–65.5 wt%, SiO_2 = 33–34 wt%, $Fe_2O_3 \leq 0.10$ wt% and $TiO_2 \leq 0.15$ wt%, mean diameter (D_{50}) of 1.5 μm, specific gravity of 4.6 g/cm^3 and melting point of 2200 °C (Kreutzonit Super, Mahlwerke Kreutz, Germany). The second starting powder was monoclinic zirconia (m-ZrO_2) with specific area of 14 m^2/g and mean diameter (D_{50}) of 0.2 μm and 99.97% purity (TZ-0 Tosoh Co., Ltd. Japan).

An initial pre-mixture of powders (20 vol.% ZrO_2) was carried out in ethanol, and then this powder mixture was milled. In order to enhance the SPS kinetics, the powder mixture with high surface activation was dryly milled using a high energy planetary mill (7 Premium Line, Fritsch Co., Ltd., Germany) this volume proportion was probed to be suitable for other particulate reinforced zircon materials.[19,27] To minimize contamination during the HEBM the jar and milling media employed were made of zirconia; 85 ml zirconia jars were used with 60 g of zirconia balls (3 mm diameter) as milling media; the ratio between the weight of powder and the milling balls was 1:10 in each batch.[24] A 900 rpm rotation speed was used; in these conditions the milling is so energetic that the jars were left to cool down for 90 min every 5 min of HEBM.

Densification of the ball milled powders was conducted using a SPS machine (SPS-1050, Sumitomo, Kawasaki, Japan). Detail information about the equipment and the sintering procedure can be found elsewhere.[13] The powder was placed into a graphite die with an inner diameter of 10 mm; 1.0 g of milled zircon powder was poured into the die.

The temperature was measured accurately using a pyrometer focused on the die surface of the inner die (i.e., 1 cm far from the sample). Graphite felt was used to reduce the heat loss by radiation. The powder was heated from room temperature up to 700 °C for 10 min, subsequently, up to the sintering temperature (1200, 1300, 1400 and 1500 °C). Materials were named Z12, Z13, Z14 and Z15 respectively. The dwelling time was 10 min and 100 MPa pressure was raised just after the beginning of the dwelling time. In order to achieve full dense sample at lower sintering temperature longer dwelling time (between 10 and 60 min) were attempted.

Density and apparent porosity of the sintered samples were evaluated by the Archimedes method. The phase composition of the ball-milled powders and of the SPSed specimens was determined by X-ray diffraction (XRD) using CuKα radiation operating at 40 kV and 300 mA. The powders morphology observations were conducted by scanning electron microscopy (SEM) and for the materials characterization (Joel, JSM-6500F, Japan and Hitachi, Miniscope TM 3000, Japan, respectively). The surfaces of the specimens were polished with diamond slurries of 15, 9, 6, 3, 1 and 0.25 μm diameter.

Vickers hardness (Hv) and fracture toughness (K_{IC}) of the obtained ceramics was evaluated with a Vickers indentation machine (Akashi AVK-A, Japan) at least six indents under 5 kg for each sample were performed. The fracture toughness (K_{IC}) was calculated by the following equation[33,34]:

$$K_{IC} = \delta\left(\frac{E}{H}\right)^{1/2}\frac{P}{c^{3/2}}$$

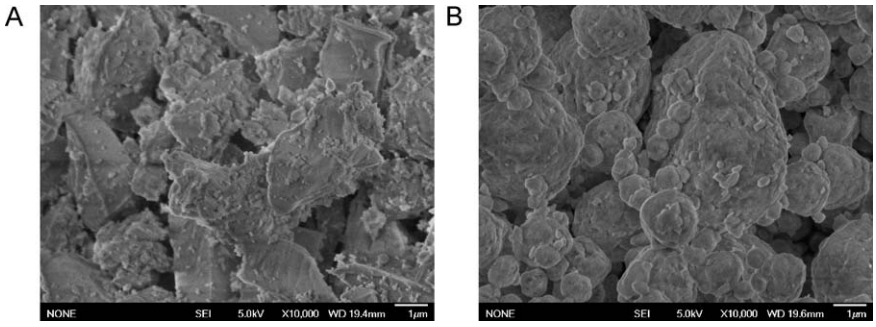

Fig. 1. SEM image (10,000×) of the powder: (A) after the pre-mixing in ethanol; (B) after the HEBM (60 min).

where E is the elastic modulus (240 GPa for zircon), H is the Vickers hardness, P is the indentation test load and c is the indentation crack length. Finally δ is a material-dependent constant that was assumed to be 0.018. The crack lengths were measured immediately after the indentation in order to avoid slow crack growth after removing the load.

3. Results and discussions

3.1. High energy ball milling (HEBM)

Fig. 1A shows the SEM image (5000×) of the pre-mixed zircon zirconia mixture before the high energy milling treatment. Zircon particles, with sharp edges and particle sizes between 3 and 1 μm, are fully covered by the nano sized zirconia (≈100 nm) particles which are highly agglomerated in sub-micron size aggregates.

Fig. 1B shows the SEM image of the mixture after 60 min of HEBM. Even if the particle size was no significantly reduced the powder morphology was modified. Rounded zircon particles can easily observed; moreover the small zirconia agglomerations cannot clearly detected, hence it can assumed that they are covering the surface of the zircon particles due to the mechanical treatment, the latter hypothesis is verified in Section 3.2. Perhaps longer or more energetic (increasing the milling media size or the milling time[9]) mechanical treatments could introduce a decrease in particle size. The main objective of the present investigation was (i) to achieve highly homogeneous mixture of the starting powders; (ii) promote the sintering kinetic activation as demonstrated for pure zircon material.[13]

Fig. 2 shows the XRD patterns of the mixtures before and after the milling treatment. The only crystalline phases detected, as expected, were zircon and monoclinic zirconia, the lost of crystallinity was not significant for the zircon crystals although the peaks intensities decreased (50% after 60 min) due to the HEBM treatment. As consequence of the mechanical ball impacts during the HEBM, the principal peaks of m-ZrO_2 (inset in Fig. 2) decreased in intensity and showed a significant peak broadening attributed to both the decrease in crystallinity and the crystallite size reduction.

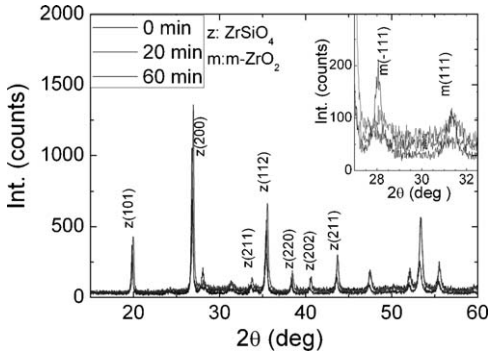

Fig. 2. XRD Patterns of the starting powders before and after the HEBM.

3.2. SPS sintering and microstructural evolution

The 60 min milled powder mixture was spark plasma sintered. Powders were heated at a high heating rate (100 °C/min) up to the preset sintering temperatures between 1200 °C and 1500 °C. Before the holding time the pressure (100 MPa) was raised at the rate of about 3 MPa/s. Materials were called Z12, Z13, Z14 and Z15 depending on the sintering temperatures 1200 °C, 1300 °C, 1400 °C and 1500 °C respectively.

The final density and apparent porosity of the materials obtained are plotted as a function of the sintering temperature in Fig. 3. As expected, the density increased with the temperature. The density of sample sintered at 1300 °C was over 4.7 g/cm^3 which corresponded to almost 98% of the theoretical value.

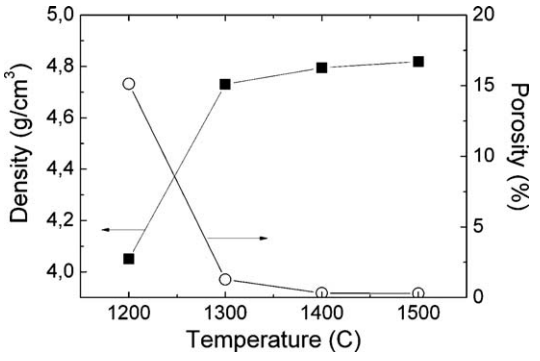

Fig. 3. Density and apparent porosity as a function of the sintering temperature (10 min dwelling).

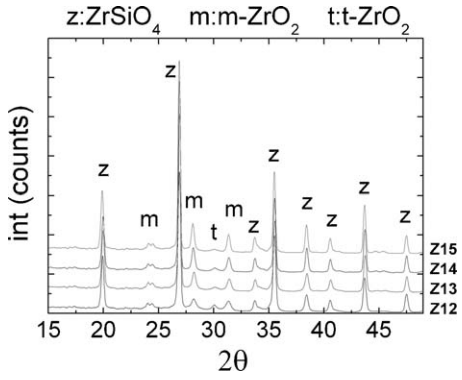

Fig. 4. XRD Patterns of the zircon zirconia composites.

The porosity was lowered down to less than 1% for the sample sintered at 1400 °C which corresponded to 99% of the theoretical zircon–zirconia (20 vol.%) density. The sample Z15 (1500 °C) achieve near full densification. The combination of SPS and HEBM, in comparison with convention sintering process (1600 °C) employing unmilled powder,[14,16,17] permitted to lower the conventional sintering temperature by 200 °C. In contrast to the pure zircon material,[13] the addition of the nano sized zirconia enhanced the sintering. At given constant sintering conditions as 1300 °C, 10 min holding, and 100 MPa the pure zircon material was 8% porous, on the contrary, the nano-zirconia addition lowered the porosity down to 2%.

Fig. 4 shows the XRD patterns of the sintered samples Z12–15. The principal crystalline phases, as expected, are zircon and m-zirconia. The t-zirconia principal diffraction peak (1 0 1) was detected with low intensities. The content of t-zirconia, estimated as proposed by Toroya et al.,[35] was in all the cases below the 10% of the total zirconia.

It was impossible to differentiate between the zirconia resulting from the dissociation and the one from the starting powder mixture. Similarly the zircon dissociation cannot be quantified by XRD. However it might be detected by SEM due to the different morphology between the zirconia grains resulting from the dissociation and the ones in the initial powder.

Fig. 5A shows typical SEM images of the Z13 sample sintered at 1300 °C. The microstructure consists of a homogeneous distribution of rounded zircon grains (gray) with a mean diameter between 2 and 4 μm surrounded at the grain boundary by a continuous zirconia matrix (white) with thickness below 0.5 μm. Although some pore can be observed (black), the material appear as dense as shown in Fig. 3. The grain growth was minimized by the short holding time and by the rapid heating rate (100 °C/min). As described in Fig. 1B, after the HEBM, the nanograins zirconia formed a submicronic layer on the surface of the zircon particles. The high pressure (100 MPa) and the elevated temperatures (1300 °C) together with the electrical current of the SPS processes are suitable conditions to achieve the near full densification of the milled powders. The shape and size of the zircon grains did not changed significantly after the sintering.

As shown in Fig. 5B, the microstructural configuration of the material sintered at 1400 °C (Z14), is similar to the Z13, no change in the zircon grain size was observed. In agreement with

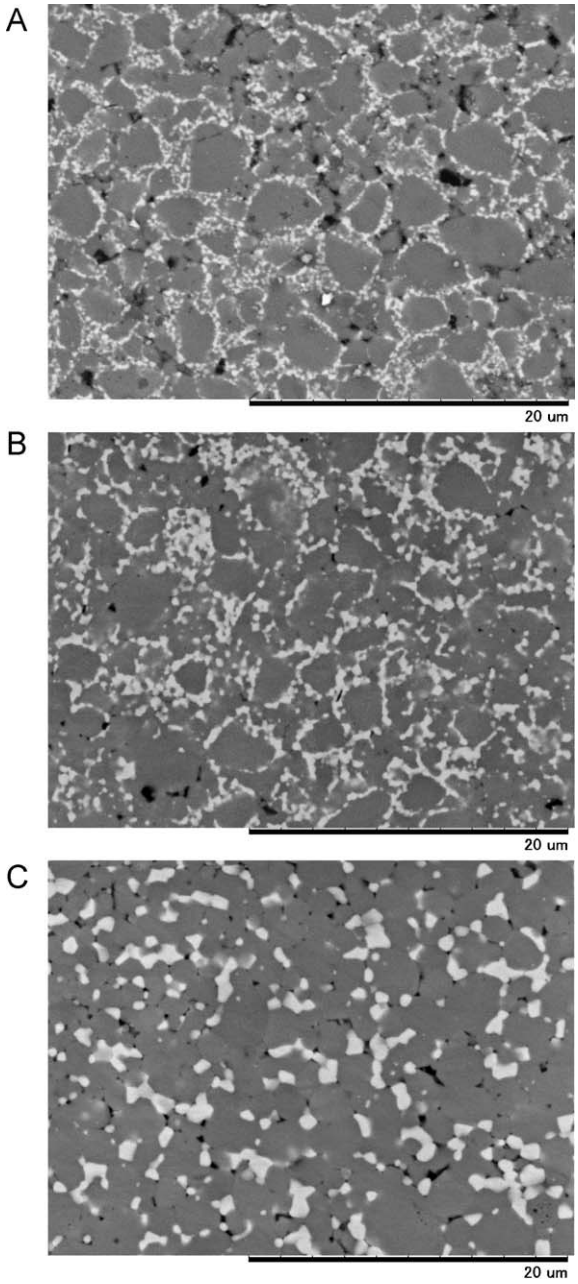

Fig. 5. SEM images: (A) Z13 material, (B) Z14 material and (C) Z15 material.

data plotted in Fig. 3, the porosity is lower than the sample Z13 one.

Finally, Fig. 5C shows the typical microstructure of the Z15 sample sintered at 1500 °C, the microstructural configuration differs from the one of Z13 and Z14 samples. It consists of a continuous zircon matrix with well dispersed intergranular zirconia grains. The zircon grain sizes remain almost unchanged but the zirconia grains size increased considerably up to 1 and 2 μm. The zirconia grains are preferentially located at the zircon grain boundaries. By increasing the sintering temperature, the nano sized zirconia grains coalesced during the sintering at 1500 °C.

The concurrent effects of the powder mechanical activation and the current activation sintering process may explain the

Table 1
Processing variables, sintering parameters, Vickers hardness and fracture toughness of the materials processed with different dwelling time.

Sample	Sintering temperature (°C)	Dwelling time (min)	Density (g/cm^3)	Porosity (%)	Hv (kg/mm^2)	K_{IC} (MPa m$^{1/2}$)
Z13	1300	10	4.72	1.29	1304 (230)	3.02 (0.23)
Z13–30	1300	30	4.73	0.34	1391 (150)	2.80 (0.16)
Z13–60	1300	60	4.80	0.26	1522 (180)	2.77 (0.16)

lower sintering temperature in comparison with the hot pressing or pressureless sintering.[13] The interlocking configuration (Fig. 5C) might enhance the mechanical properties of these materials (this as confirmed in Section 3.3).

At last, no dissociated zirconia grains were detected in the Z15 microstructure, the presence of nanozirconia depressed the zircon thermal dissociation that was observed in the case of a pure zircon material processed in equivalent conditions.[13]

In summary, two microstructural configurations were obtained by controlling the sintering temperature of the SPS processing.

3.3. Dwelling time influence

The influence of the dwelling time, in the range 10–60 min, was investigated. Table 1 summarizes the effect of the SPS dwelling at 1300 °C on the porosity and the density of the material. Microstructure evolution is shown in Fig. 6A–C, for 10, 30 and 60 min respectively, these are SEM images of the polished surfaces.

By extending the holding time, the porosity decreased to less than 0.4% which correspond to 4.8 g/cm^3 absolute density. The outstanding densification, obtained at such low temperature for zircon materials, highlights the benefits of the developed processing route. The microstructural configuration and the crystalline phases are comparable to the Z13 and Z14 samples (Fig. 5A and B). The XRD patterns, showed in Fig. 4, evidence the zircon as main crystalline phase together with monoclinic zirconia. On the contrary respect to the high temperature (1500 °C), the dwelling time did not generated any changes in the microstructural configuration. Both the samples S13–30 and S13–60 exhibits the "low temperature" configuration of nanoziroconia acts as a bonding phase. By increasing the holding time the SEM images show a progressive the decrease in porosity, measured by immersion method (Table 1), as observed in the SEM images (Fig. 6B and C).

3.4. Hardness and fracture toughness

Toughening enhancement can be obtained by incorporating zirconia (ZrO_2) particles in a ceramic matrix.[29–31] Several concurrent mechanisms are involved in the toughening: stress-induced transformation, microcraking, crack bowing and crack deflection and also the thermal expansion mismatch. However, as the content of tetragonal zirconia is negligible, the transformation toughening mechanism should be discarded. In all cases, the operative toughening mechanism depends on the matrix stiffness, zirconia particle size, chemical composition and testing temperature.[29–31] The different microstructural configurations affected significantly the mechanical properties.

The hardness and the bending strength as a function of the sintering temperature are plotted in Fig. 7. Both properties

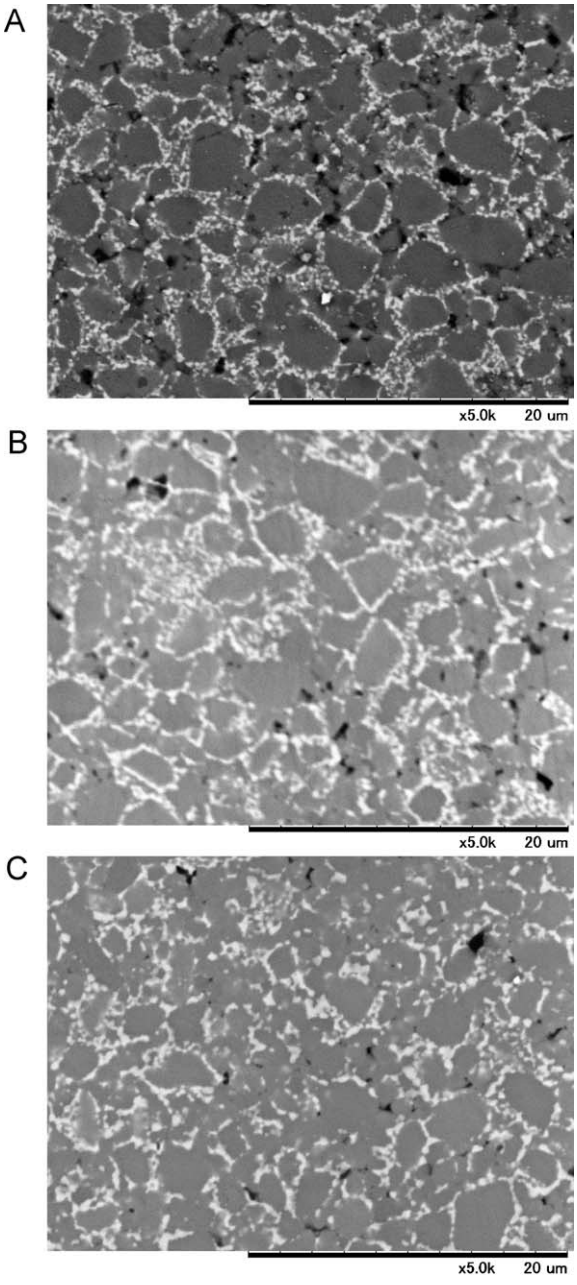

Fig. 6. SEM images of the materials as a function of the soaking time of the SPS processes at 1300 °C with 100 MPa of pressure: (A) 10 min (Z13), (B) 30 min (Z13–30) and (C) 60 min (Z13–60).

Table 2
Comparison of material toughness (K_{IC}) with the data reported in literature.

Reference	Configuration	Additive	Proportion	Processing conditions	K_{IC} (MPa m$^{-1/2}$)	
					Monolithic zircon	Reinforced zircon
[27]	Dispersed	Mullite	15 wt.%	Presureless 1600 °C 2 h	1.8	2.0
[19]	Dispersed	SiC	20 vol.%	Hot pressing 1600 °C 1 h 25 MPa	3.0	3.8
[19]	Dispersed	TiC	20 vol.%	Hot pressing 1600 °C 1 h 25 MPa	3.0	4.5
[23]	Dispersed	2Y-TZP	10–30 vol.%	Hot pressing 1600 °C 1 h 25 MPa	3.0	4.3
[25]	Whiskers	SiC	20 vol%	Hot pressing, synthetic powders 1650 °C 1 h 30 MPa	2.0	4.0
[26]	Whiskers + dispersed	SiC (w) + 2Y-TZP	10–40 vol.%	Hot pressing, synthetic powders 1600 °C 1 h 30 MPa	3.0	4.0–7.0
This study	Bonding phase	m-ZrO_2	20 vol.%	SPS of mechanically activated commercial powders 1400 °C 10 min	3.0	3.6
This study	Dispersed	m-ZrO_2	20 vol.%	SPS of mechanically activated commercial powders 1500 °C 10 min	3.5	4.0

increased with the sintering temperature. The full densification was achieved at 1400 °C, no increase in the hardness was observed above such temperature.

As the Hv the fracture toughness depended strongly with the sintering temperature. The K_{IC} value increased with the densification (Z12–Z14). The Z15 sample, which exhibits dispersoidal configuration, posses the highest toughness among the manufactured samples.

Table 1 shows Hv and K_{IC} evaluated for the materials obtained at 1300 °C with different soaking times. Hardness grows with the densification of these materials. However, the K_{IC} progressively lowered by extending the holding time. This fact makes clear that the enhancement in the fracture toughness is related more to the microstructural configuration change rather to the densification.

In comparison with previously reported literature data for the monolithic zircon (1000–1300 kg/mm^2 and 2–3 MPa m$^{1/2}$),[13,14] the hardness and fracture toughness could be raised up to ≈1500 kg/mm^2 and ≈4.0 MPa m$^{1/2}$, which corresponded to a relative enhancement of 15% and 30% respectively. The advanced processing routes HEBM together with SPS can be used for the manufacturing of zircon materials with superior mechanical properties.

In Table 2 the materials obtained are compared with the data reported in literature for dense zircon materials reinforced with different second phases.

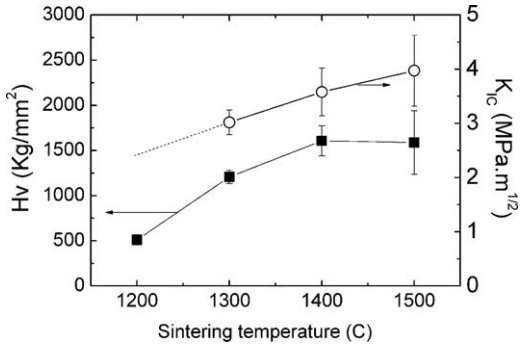

Fig. 7. Vickers hardness (Hv) and fracture toughness (K_{IC}) of the processed materials.

The fracture toughness of the materials obtained is comparable with the hot pressed 2Y-TZP and SiC dispersoidal reinforced zircon material, slightly lower than the hot presses TiC dispersoidal zircon material. Finally the toughness achieved by more tailored microstructures like whiskers and fibres reinforcements was not achieved by the two microstructural configurations accomplished in this study. It is important to point out that the corrosion resistance is not affected by the zirconia incorporation. It is also important to take into account that this material was processed from commercial powders and not from chemical precursors.

4. Conclusions

- Dense zircon ($ZrSiO_4$)–zirconia (20 vol.%) (m-ZrO_2) composite ceramics were obtained from mechanically activated commercial powders and spark plasma sintering (SPS) without any sintering additive at low temperatures and short time.
- The high energy ball milling (HEBM) was a successful pretreatment for obtaining highly homogeneous nano particle mixtures. Furthermore the HEBM powder activation enhanced the SPS sintering kinetics.
- Unlike conventional sintering processes, the highly level of density was achieved by SPS at low temperatures (1300–1400 °C) and short holding time.
- The thermal zircon dissociation was not observed, it was depressed by the presence of zirconia nano grains.
- Two different microstructural configurations of dense zircon–zirconia ($ZrSiO_4$–ZrO_2) ceramic composites were obtained. In the first configuration the nano sized zirconia particles (100 nm) act as a continuous phase surrounding the round micronic (2–3 μm) zircon grains. In the second one, a continuous zircon phase with well distributed dispersed zirconia grains was achieved. The microstructure configuration was controlled by the sintering parameters. The first one was achieve at the lower temperature programs regardless the dwelling time. The second resulted from the high temperature sintering (1500 °C). Both configurations presented better fracture toughness and Vickers hardness if compared

to the pure zircon material processed obtained under the same conditions.

- The high temperature configuration (1500 °C) led to augmented fracture toughness (4.0 MPa $m^{1/2}$), evidencing that the zirconia reinforcement mechanisms are more efficient in the dispersoidal configuration.

References

1. Niihara K. New design concept of structural ceramics. Ceramic nanocomposites. *Journal of the Ceramic Society of Japan* 1991;**99**(1154):974–82.
2. Sternitzke M. Structural ceramic nanocomposites. *Journal of the European Ceramic Society* 1997;**17**(9):1061–82 [Review].
3. Ohji T, Jeong YK, Choa YH, Niihara K. Strengthening and toughening mechanisms of ceramic nanocomposites. *Journal of the American Ceramic Society* 1998;**81**(6):1453–60.
4. Omori M. Sintering, consolidation, reaction and crystal growth by the spark plasma system (SPS). *Materials Science and Engineering A* 2000;**287**(2):183–8.
5. Orru R, Licheri R, Locci AM, Cincotti A, Cao G. Consolidation/synthesis of materials by electric current activated/assisted sintering. *Materials Science and Engineering R: Reports* 2009;**63**(4–6):127–287.
6. Grasso S, Sakka Y, Maizza G. Electric current activated/assisted sintering (ECAS): a review of patents 1906–2008. *Science Technology and Advanced Materials* 2009;**10**:053001.
7. Sakka Y. Fabrication of highly microstructure controlled ceramics by novel colloidal processing. *Journal of the Ceramic Society of Japan* 2006;**114**(1329):371–6.
8. Suárez G, Sakka Y, Suzuki TS, Uchikoshi T, Aglietti EF. Effect of bead-milling treatment on the dispersion of tetragonal zirconia nanopowder and improvements of two-step sintering. *Journal of the Ceramic Society of Japan* 2009;**117**(1364):470–4.
9. Suryanarayana C. Mechanical alloying and milling. *Progress in Materials Science* 2001;**46**(1–2):1–184.
10. Zhan GD, Kuntz JD, Wan J, Mukherjee AK. Single-wall carbon nanotubes as attractive toughening agents in alumina-based nanocomposites. *Nature Materials* 2003;**2**(1):38–42.
11. Zhan GD, Kuntz JD, Wan J, Garay J, Mukherjee AK. A novel processing route to develop a dense nanocrystalline alumina matrix (<100 nm) nanocomposite material. *Journal of the American Ceramic Society* 2003;**86**(1):200–2.
12. Morita K, Hiraga K, Kim BN, Yoshida H, Sakka Y. Synthesis of dense nanocrystalline ZrO_2–$MgAl_2O_4$ spinel composite. *Scripta Materialia* 2005;**53**(9):1007–12.
13. Rendtorff NM, Grasso S, Hu C, Suarez G, Aglietti EF, Sakka Y. Dense zircon ($ZrSiO_4$) ceramics by high energy ball milling and spark plasma sintering. *Ceramics International* 2011;(October), doi:10.1016/j.ceramint.2011.10.001.
14. Mori T, Yamamura H, Kobayashi H, Mitamura T. Preparation of high-purity $ZrSiO_4$ using sol–gel processing and mechanical properties of the sintered body. *Journal of the American Ceramic Society* 1990;**75**(9):2420–6.
15. Moreno R, Moya JS, Requena J. Slip casting of zircon by using an organic surfactant. *Ceramics International* 1991;**17**(1):37–40.
16. Garrido LB, Aglietti EF. Zircon based ceramics by colloidal processing. *Ceramics International* 2001;**27**(5):491–9.
17. Shi Y, Huang X, Yan D. Fabrication of hot-pressed zircon ceramics: mechanical properties and microstructure. *Ceramics International* 1997;**23**(5):457–62.
18. Carbonneau X, Hamidouche M, Olagnon C, Fantozzi G, Torrecillas R. High temperature behaviour of a zircon ceramic. *Key Engineering Materials* 1997;**132–136**:571–4.
19. Shi Y, Huang X, Yan D. Mechanical properties and toughening behavior of particulate-reinforced zircon matrix composites. *Journal of Materials Science Letters* 1999;**18**(3):213–6.
20. Singh RN. High-temperature mechanical properties of a uniaxially reinforced zircon–silicon carbide composite. *Journal of the American Ceramic Society* 1990;**73**(8):2399–406.
21. Singh RN. Mechanical properties of a zircon matrix composite reinforced with silicon carbide whiskers and filaments. *Journal of Materials Science* 1991;**26**(7):1839–46.
22. Singh RN. SiC fibre-reinforced zircon composites. *American Ceramic Society Bulletin* 1991;**70**(1):55–6.
23. Shi Y, Huang X, Yan D. Toughening of hot-pressed $ZrSiO_4$ ceramics by addition of Y-TZP. *Materials Letters* 1998;**35**(3–4):161–5.
24. Alahakoon WPCM, Burrows SE, Howes AP, Karunaratne BSB, Smith ME, Dobedoe R. Fully densified zircon co-doped with iron and aluminium prepared by sol–gel processing. *Journal of the European Ceramic Society* 2010;**30**(12):2515–23.
25. Kondoh I, Tanaka T, Tamari N. Sintering of zircon–silicon carbide whisker composites and their mechanical properties. *Journal of the Japanese Ceramic Society* 1993;**101**(3):369–72.
26. Shi Y, Huang X, Yan D. Synergistic strengthening and toughening of zircon ceramics by the additions of SiC whisker and 3Y-TZP simultaneously. *Journal of the European Ceramic Society* 1997;**17**:1003–10.
27. Rendtorff NM, Garrido LB, Aglietti EF. Mechanical and fracture properties of zircon–mullite composites obtained by direct sintering. *Ceramics International* 2009;**35**(7):2907–13.
28. Rendtorff NM, Garrido LB, Aglietti EF. Zirconia toughening of mullite–zirconia–zircon composites obtained by direct sintering. *Ceramics International* 2010;**36**(2):781–8.
29. Zender H, Leistner H, Searle H. ZrO_2 materials for applications in the ceramic industry. *Interceramics* 1990;**39**(6):33–6.
30. Jin X. Martensitic transformation in zirconia containing ceramics and its applications. *Current Opinion in Solid State & Materials Science* 2005;**9**(6):313–8.
31. Kelly PM, Francis Rose LR. The martensitic transformation in ceramics—its role in transformation toughening. *Progress in Materials Science* 2002;**47**(5):463–557.
32. Claussen N, Jahn J. Mechanical properties of sintered in situ-reacted mullite–zirconia composites. *Journal of the American Ceramic Society* 1980;**63**(3–4):228–9.
33. Miyazaki H, Hyuga H, Yoshizawa Y, Hirao K, Ohji T. Measurement of indentation fracture toughness of silicon nitride ceramics: I. Effect of microstructure of materials. *Key Engineering Materials* 2007;**352**: 41–4.
34. Niihara K, Morena R, Hasselman DPH. Evaluation of K_{IC} of brittle solids by the indentation method with low crack-to-indent ratios. *Journal of Materials Science Letters* 1982;**1**(1):13–6.
35. Toraya H, Yoshimura M, Somiya S. Calibration curve for quantitative analysis of the monoclinic-tetragonal ZrO_2 system by X-ray diffraction. *Journal of the American Ceramic Society* 1984;**67**:C119–21.